

# Vulnerability of roofing components to wind loads

N.C. Jayasinghe\* and J.D. Ginger

*Cyclone Testing Station, School of Engineering and Physical Sciences, James Cook University, Townsville, QLD 4811, Australia*

*(Received October 15, 2010, Accepted December 23, 2010)*

**Abstract.** The vulnerability of roofing components of contemporary houses built in cyclonic regions of Australia is assessed for increasing wind speeds. The wind loads and the component strengths are treated as random variables with their probability distributions derived from available data, testing, structural analysis and experience. Design details including types of structural components of houses are obtained from surveying houses and analyzing engineering drawings. Wind load statistics on different areas of the roof are obtained by wind tunnel model studies and compared with Australian/New Zealand Standard, AS/NZS 1170.2. Reliability methods are used for calculating the vulnerability of roofing components independently over the roof. Cladding and batten fixings near the windward gable edge are found to experience larger negative pressures than prescribed in AS/NZS 1170.2, and are most vulnerable to failure.

**Keywords:** vulnerability; reliability; wind loads; houses; wind tunnel; strength; probability.

---

## 1. Introduction

The large scale damage to housing in windstorms identifies the need for understanding their response to wind loads and developing methods for assessing vulnerability in order to mitigate wind damage. There is a wide range of house types with differences in size, shape, potential openings in envelope, cladding, roof shape and pitch, method of construction, structural system and age. The resistance of a house structure to wind loading depends on the effect of these features on the wind pressures experienced and the strength of its components and connections.

The assessment of the vulnerability of houses to windstorms requires knowledge in analyzing uncertainties occurring due to load actions and building response. There are basically two types of uncertainties. First is the variability of factors that are inherent to wind load and component resistance. The other type occurs due to inadequate knowledge - such as the use of incorrect assumptions, incomplete databases or incorrect data for probabilistic assessment, use of incorrect analysis methods etc. Houses are complex structures with many load sharing components, making it difficult to quantify the resistance of each component especially as the availability of full scale data is limited. This study uses statistical parameters to account for the uncertainty and variability associated with loads and component strength.

Windstorm damage surveys reveal that roofing components are the most vulnerable part of a

---

\* Corresponding Author, Mr., E-mail: [nandana.jayasinghe@my.jcu.edu.au](mailto:nandana.jayasinghe@my.jcu.edu.au)

house. Damage surveys (Walker 1975) and full scale data from the Cyclone Testing Station have shown that the typical modes of roofing failure of houses to wind loading are associated with the strength capacity of the joints between components being exceeded. Therefore, the wind loads acting on different components over a roof associated with the direction of the incident wind, need to be found. In this paper, a wind tunnel study on a typical house type selected from a recent survey is carried out to determine the wind loads acting on roofing connections over several regions of the roof. The probability distributions of the strength of typical components used in these contemporary houses are determined and combined with the wind loads to identify most vulnerable components in various regions of the roof.

Wind loads acting on the roof cladding are transferred via the supporting structure and the walls to the foundation. Three connection types that are directly involved in this load transfer path on contemporary houses are roof cladding connection to batten, batten to truss connection and truss to wall connection. This study analyses these connections and determines their strength capacities in probabilistic terms from available data, testing, structural analysis and experience. In this study, the vulnerability of each of these components is given by its probability of failure for a given wind speed. The vulnerability of each connection type is determined by using reliability methods incorporating probability theory and reliability concepts used by Holmes (1985), Leicester *et al.* (1985), Pham (1985), Melchers (1985) and Tang and Melchers (1985).

Vulnerability studies by Walker (1995) have produced empirical damage curves that are used for estimating the damage and loss for pre-1980 and post-1980 houses built in cyclone regions of Australia. Henderson and Ginger (2007) studied the vulnerability of a high-set 1960s house, with a low-pitch gable roof built in the northern part of Australia, to wind speeds experienced in tropical cyclones by using reliability concepts. Studies by Rosowsky and Ellingwood (2002), Ellingwood *et al.* (2004), Pinelli *et al.* (2004), Lee and Rosowsky (2005), Li and Ellingwood (2006) have assessed the vulnerability of residential construction in the US to wind loading using reliability methods and probability techniques.

## 2. Reliability analysis

The basic framework for probability based design is provided by reliability theory. In this approach, the load and the resistances are taken as random variables and the required statistical information is assumed to be available. In this process, the load effect,  $S$  and structural resistance,  $R$  are analyzed statistically and the probability of failure calculated. The information required are the mean and coefficient of variation (COV) values of  $S$  and  $R$  or their probability density functions  $f_S(S)$  and  $f_R(R)$ . The dispersion or widths of the two distributions represent the uncertainty in  $S$  and  $R$ , and can be given with a coefficient of variation or standard deviation. Failure occurs when the load effect exceeds the resistance of the component ( $S > R$ ). This approach can be used for estimating the vulnerability of house components to wind loading as shown by Henderson and Ginger (2007).

Assuming that  $S$  and  $R$  are statistically independent, the probability of failure is given by

$$p_f = \int_{-\infty}^{\infty} F_R(S) f_S(S) dS \quad (1)$$

where  $F_R(R)$ , is the cumulative probability distribution, such that

Rosowsky and Cheng (1999) studied the reliability of roof system components in light frame construction in the US subjected to high wind uplift loads. The reliability method described here was used for evaluating the performance of roofing components for three coastal residential structures. The results of their study identified a relatively small number of connections that dominate the modes of failure of these house types.

### 3. Roof structural system

A survey was carried out recently in the cyclonic region of Northern Australia to determine the structural characteristics of contemporary houses under construction. The features such as size, shape, potential openings in envelope, cladding, roof shape and pitch, method of construction, type of connections and structural system were surveyed. In addition the approved drawings for each house submitted to the local authorities were also reviewed. It was found that more than 90% of the 100 houses surveyed were masonry block type. Figs. 1(a) and 1(b) show a typical masonry house with gable roof shape and roofing connections. The walls are constructed from masonry blocks filled with concrete and continuous reinforcements at regular intervals. The roof structure consists of timber trusses and top hat battens clad with metal roof sheeting. The timber trusses are manufactured from machine grade pine (MGP12) components joined with toothed truss connector metal plates and connected to the bond beam at the top of the wall with a metal cleat bolted to the truss. Sometimes straps are used to connect the truss to the wall instead of cleats. Top hat battens manufactured from G550 steel with a base metal thickness (BMT) of 0.75 mm are fixed to the top chord of these trusses with two Type-17 screws (No14-10 × 25 mm). The metal roof cladding is usually corrugated profile with a base metal thickness of 0.42 mm and is attached to the battens using Type-17 cladding fasteners (No14-10 × 50 mm) without cyclone washers. The spacing of the cladding fasteners is 152 mm but sometimes different spacings are used in the edges and middle of the roof. Ceiling sheeting (usually plasterboards) is fixed directly to the trusses or to metal ceiling battens connected to the bottom chord of trusses. Contemporary houses typically have either gable or hip roofs or a combination of these. Based on the survey data, a gable end 10 m × 19.8 m × 2.7 m low rise house with 0.6 m roof overhang and 22.5° pitch, shown in Fig. 2 represents a typical contemporary house.

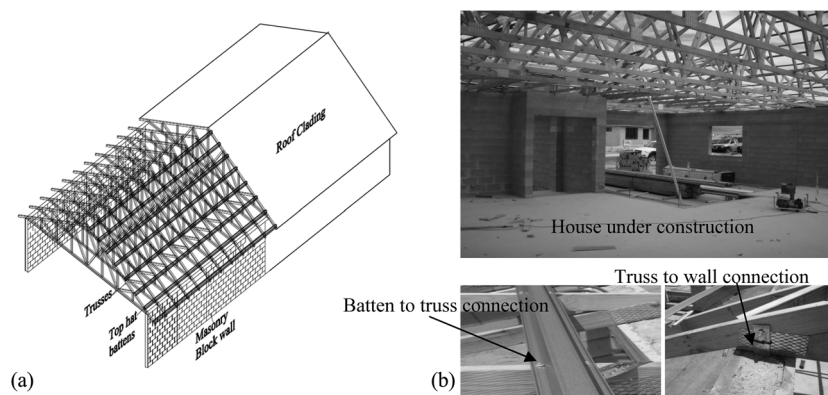


Fig. 1(a) House with masonry walls and (b) Trusses and batten connections

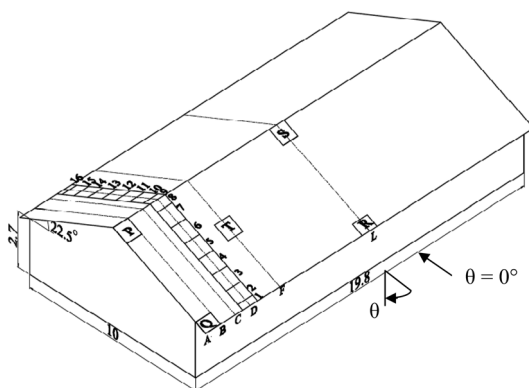


Fig. 2 10 m  $\times$  19.8 m  $\times$  2.7 m gable-end low-rise house with 22.5° roof pitch

#### 4. Loads

The Building Code of Australia (Australian Building Codes Board 2010) provides the regulatory framework for the design of most buildings including contemporary houses, in Australia. The Australian Standard for Wind Actions, AS/NZS 1170.2 (2002) referenced by the BCA, specifies the design wind loads. The ‘wind loads for housing’ Standard AS 4055-2006, “based on AS/NZS 1170.2”, is used for assessing wind loads on contemporary housing. Design wind pressures acting on the roofs of houses are dependent on their geometries, as shown in AS/NZS 1170.2 (2002). These pressures are obtained from wind tunnel studies, such as those by Holmes (1981) and Xu and Reardon (1998), who have presented wind pressures on low rise houses with hip and gable roofs with a range of slopes. In addition, there is a large variability associated with the pressures especially near roof corners, where the most severe wind loading normally occurs. Several studies have been carried out to assess the variation of wind loads on roof corners (Lin and Surry 1998) and the influence of roof eaves (over hang) on the characteristics of pressures.

Previous studies have investigated the probability distributions of extreme local pressures on buildings. Holmes and Cochran (2003) used several thousand extreme pressure coefficients from repeated time history samples from a wall tap and a roof tap on a model of the Texas Tech University Test Building to determine the appropriate probability distributions for the data. Both the Type I (Gumbel) Extreme Value Distribution, and the Generalized Extreme Value Distribution were used to fit the data. Li *et al.* (2009) studied a similar type of full scale building and found that the Type III Extreme Value Distribution matched the data measured on a roof corner. Kasperski and Hoxey (2008) also found that Type III distribution can be fitted to the full scale test data from 6 m  $\times$  6 m  $\times$  6 m cube Silsoe building.

This section presents the probabilistic descriptions of wind loads on the roof of typical contemporary gable end houses. The wind loads are obtained from a wind tunnel model study on a house with dimensions based on the survey data. This section also determines the appropriate probability distribution functions of external pressures on tributary areas representing roof components.

##### 4.1. Wind tunnel model test

Wind tunnel model studies were carried out in the 2.0 m high  $\times$  2.5 m wide  $\times$  22.0 m long boundary-layer wind tunnel of the Cyclone Testing Station at James Cook University. The approach

atmospheric boundary layer, representative of suburban terrain, was simulated at a length scale of 1/50 over a fetch by using a 250 mm high trip board at the upstream end followed by an array of blocks on the tunnel floor. A model of a 10 m × 19.8 m × 2.7 m low-rise house, with 0.6 m roof overhang and a gable roof with 22.5° pitch, as shown in Fig. 2 was constructed at a length scale of 1/50. The wind loads were measured on tributary areas representing cladding fixings in regions; *P*, *Q*, *R*, *S* and *T*, and on roof trusses spaced 900 mm apart, identified as *A*, *B*, *C*, *D*, *F* and *L* shown in Fig. 2. Each roof truss tributary area was divided into sixteen panels identified as 1...16 (see Truss *D* in Fig. 2). Each panel represents a batten-truss connection tributary area. External pressures were obtained for approach wind directions  $\theta = 0^\circ$  to  $360^\circ$  in steps of  $15^\circ$ . Pressure taps on each panel were connected to a transducer using a tubing system via a pressure measurement system. The fluctuating pressures were sampled at 1250 Hertz for 30 seconds and presented as pressure coefficients ( $C_p(t) = p(t)/\frac{1}{2}\rho\bar{U}_h^2$ ). This gives a time scale of 1/20, for a length scale of 1/50 and velocity scale of 2/5, resulting in an equivalent full scale observation time of 10 minutes. These pressure coefficients were statistically analyzed to obtain mean ( $C_{\bar{p}}$ ), maximum ( $C_{\dot{p}}$ ) and minimum ( $C_{\hat{p}}$ ) pressure coefficients in a single run

$$C_{\bar{p}} = \frac{\bar{p}}{\frac{1}{2}\rho\bar{U}_h^2} \quad C_{\dot{p}} = \frac{\dot{p}}{\frac{1}{2}\rho\bar{U}_h^2} \quad C_{\hat{p}} = \frac{\hat{p}}{\frac{1}{2}\rho\bar{U}_h^2}$$

where,  $\frac{1}{2}\rho\bar{U}_h^2$  is the mean dynamic pressure at mid roof height *h*. Five runs were conducted for each angle to obtain repeat sets of pressure coefficients.

The loads on cladding fixings in regions *P*, *Q*, *R*, *S* and *T* were obtained using the individual taps in each region. The loads on batten fixings were obtained by averaging pressures acting on two or four taps over each batten-truss tributary area.

#### 4.2. Pressure distribution

The variation of external pressure coefficients  $C_{\bar{p}}$ ,  $C_{\dot{p}}$  and  $C_{\hat{p}}$  for all five runs on taps representative of cladding fixings with the wind approach direction ( $\theta$ ), for regions *P*, *Q* and *T* are shown in Figs. 3(a), (b) and (c). Wind loading standards typically provide design pressure coefficients for approach winds across and along the ridge. The nominal peak pressure coefficients ( $C_{PN}$ ) derived from Section 5 of AS/NZS1170.2 (2002) is  $C_{PN} = C_{Pe} \times K_l \times G_U^2$ , where  $C_{Pe}$  is the external pressure coefficient,  $K_l$  is the local pressure factor and  $G_U = \hat{U}_h/\bar{U}_h$  is the velocity gust factor. Here,  $\hat{U}_h$  and  $\bar{U}_h$  are gust wind speed and mean wind speed respectively at mid roof height. These  $C_{PN}$  values for each region are also shown in Figs. 3(a), (b) and (c) for wind approach directions  $0^\circ$ ,  $90^\circ$ ,  $180^\circ$  and  $270^\circ$ . These Figures show that the largest suction are expected in region *P* for wind approach directions  $135^\circ$  to  $150^\circ$ . These peak pressures exceed the design values stipulated in AS/NZS 1170.2 (2002).

The variation of area averaged external pressure coefficients  $C_{\bar{p}}$  and  $C_{\dot{p}}$  for all five runs with the wind approach direction on batten to truss panel B2, B7 and F5 are shown in Figs. 4(a), (b) and (c), respectively. These Figures show that the largest peak suction pressure occurs in regions B2 and B7 for wind approach directions  $90^\circ$  and  $135^\circ$  to  $150^\circ$  respectively. The corresponding values in AS/NZS 1170.2, for batten-to-truss connection tributary areas, are also given for wind approach directions of  $0^\circ$ ,  $90^\circ$ ,  $180^\circ$  and  $270^\circ$ .

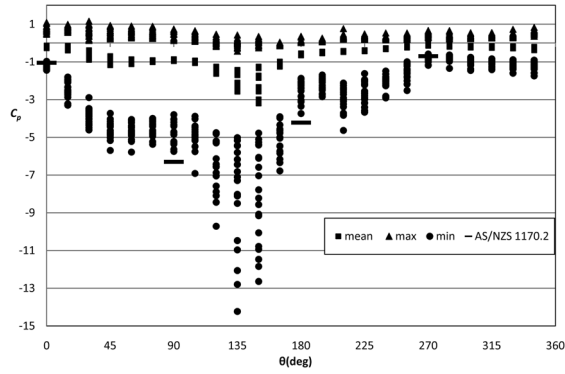


Fig. 3(a) Pressure coefficients versus wind direction -  $P$

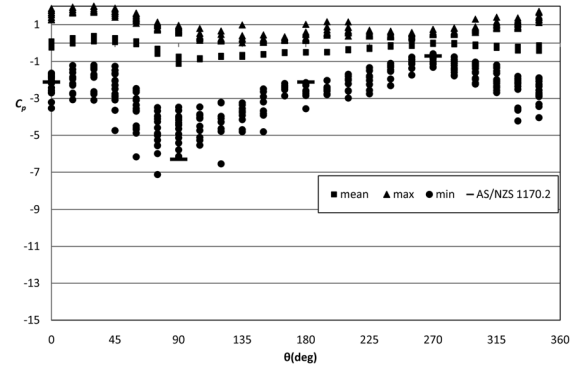


Fig. 3(b) Pressure coefficients versus wind direction -  $Q$

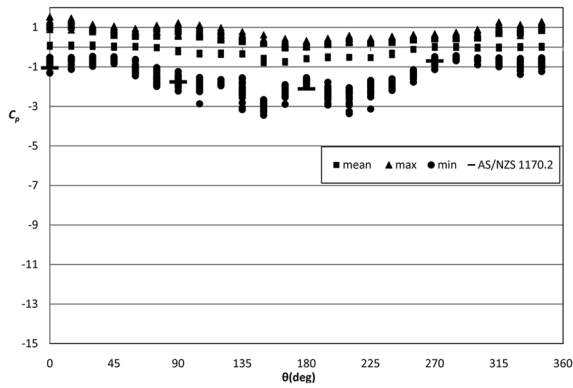


Fig. 3(c) Pressure coefficients versus wind direction -  $T$

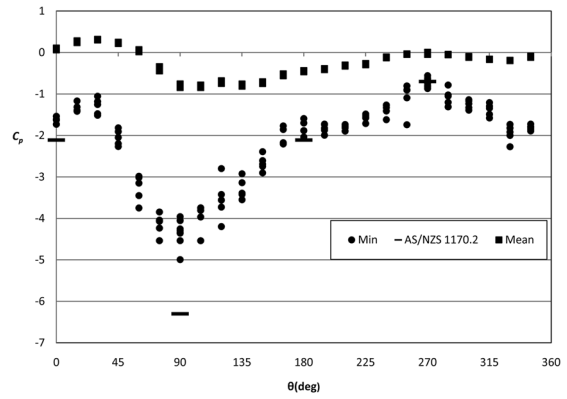


Fig. 4(a) Pressure coefficients ( $C_p$ ) versus wind direction - Batten to truss connection  $B2$

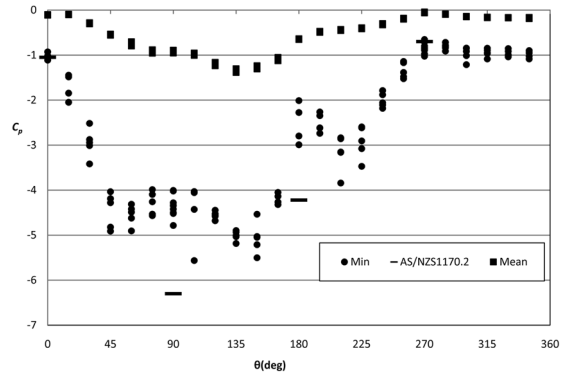


Fig. 4(b) Pressure coefficients ( $C_p$ ) versus wind direction - Batten to truss connection  $B7$

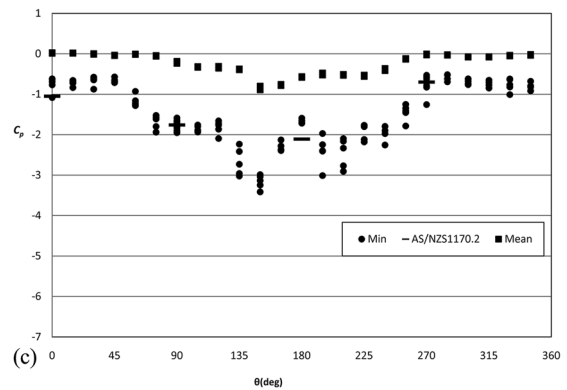


Fig. 4(c) Pressure coefficients ( $C_p$ ) versus wind direction - Batten to truss connection  $F5 T$

#### 4.3. Probabilistic distributions

The peak pressure on cladding fixing tributary area in each region is represented as normalized

Table 1 The probabilistic distribution of peak pressure ( $C_p/C_{pN}$ ) on cladding fixings at  $P$ ,  $Q$  and  $T$  regions

Approach angle ( $\theta^\circ$ )	Region $P$			Region $Q$			Region $T$		
	Mean	COV	PDF	Mean	COV	PDF	Mean	COV	PDF
0	1.16	0.11	GM	1.08	0.25	GEV	0.74	0.29	GEV
45	0.73	0.10	GEV	0.40	0.36	GEV	0.33	0.16	GEV
90	0.74	0.13	GEV	0.75	0.18	GEV	0.95	0.17	GM
135	1.25	0.36	GEV	0.62	0.13	WB	1.07	0.19	WB
180	0.60	0.21	GEV	1.23	0.17	LN	0.81	0.08	GEV
225	0.66	0.22	GEV	0.92	0.24	GEV	0.99	0.17	GEV
270	1.15	0.21	N	1.34	0.26	WB	1.06	0.24	WB
315	1.01	0.13	WB	0.94	0.24	WB	1.06	0.17	GEV

pressure coefficients ( $C_p/C_{pN}$ ) for each wind approach direction. The variation in peak pressure coefficient is described in statistical terms by fitting the data to several standard probability distribution functions (PDF) including normal (N), lognormal (LN), Rayleigh (RE), Gamma (GM), General Extreme Value (GEV) and Weibull (WB). The assumed distribution is statistically verified by goodness of fit tests. Table 1 gives the probabilistic distributions of peak pressure coefficient for cladding fixings in  $P$ ,  $Q$  and  $T$  regions for selected wind approach directions.

As described previously, the nominal pressure coefficient values are given only for wind approach directions  $0^\circ$ ,  $90^\circ$ ,  $180^\circ$  and  $270^\circ$  in AS/NZS1170.2. In order to normalize angles such as  $45^\circ$ ,  $135^\circ$ ,  $225^\circ$  and  $315^\circ$ , the highest  $C_{pN}$  value from  $\theta \pm 45^\circ$  wind approaching sector was used. For example, to normalize the wind pressure coefficients at  $45^\circ$  the higher value from  $0^\circ$  and  $90^\circ$  given in AS/NZS1170.2 was selected ( $90^\circ$  had the higher value). Similarly for  $135^\circ$ , the value given in AS/NZS1170.2 for  $90^\circ$  was used (the higher value from  $90^\circ$  and  $180^\circ$ ). These ( $C_p/C_{pN}$ ) values were used for the wind load probabilistic model described in Section 4.5 for the analysis of cladding fixings. Similarly, the probabilistic distributions for area-averaged pressures on batten to truss connection tributary areas were also found.

#### 4.4. Structural load effect on trusses

The fluctuating reaction force at the truss to wall connection shown in Fig. 5, at time  $t$  can be

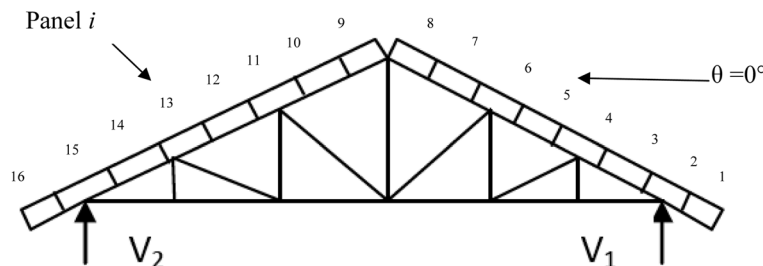


Fig. 5 Schematic diagram of roof truss showing batten to truss connection panels and truss to wall reaction forces

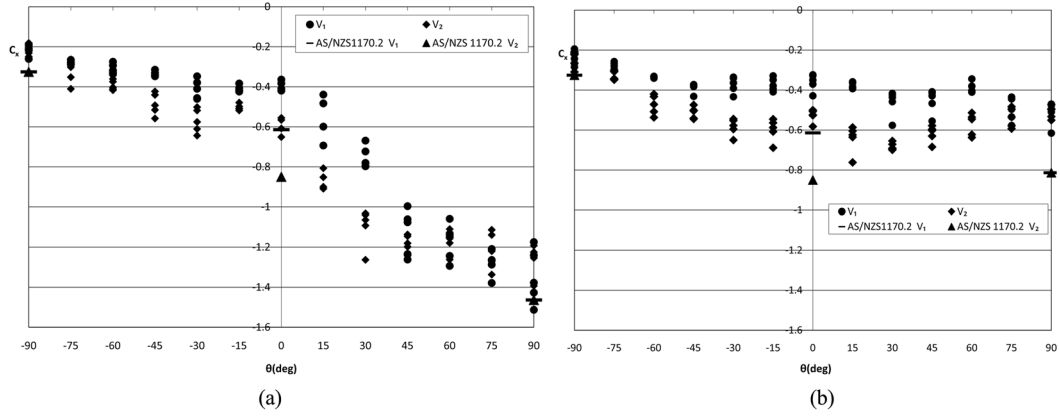


Fig. 6(a)  $\check{C}_{V1}$  and  $\check{C}_{V2}$  versus wind approach angles for Truss B and (b)  $\check{C}_{V1}$  and  $\check{C}_{V2}$  versus wind approach angles for Truss F

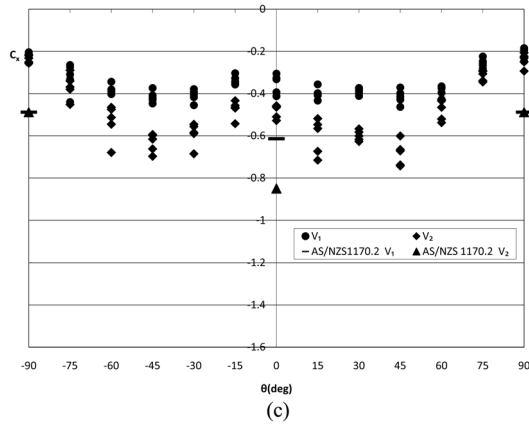


Fig. 6(c)  $\check{C}_{V1}$  and  $\check{C}_{V2}$  versus wind approach angles for Truss L

determined from Eq. (2).

$$X(t) = \sum_{i=1}^N \beta_i p_i(t) A_i \quad (2)$$

Where  $X(t)$  - the fluctuating reaction force  $V_1$  or  $V_2$ ,  $\beta_i$  - the influence coefficient for  $X$ ,  $p_i$  - wind pressure and  $A_i$  - tributary area of panel  $i$  and  $N$  - is the total number of batten to truss panels on the tributary area of the truss.

The influence coefficients for truss reaction forces  $V_1$  and  $V_2$  shown in Fig. 5 were found by placing an inward unit load at each batten to truss connection. The structural analysis package SPACE GASS version 10.81b (Integrated Technical Software 2010) was used for obtaining the reactions. These vertical reaction forces are presented in coefficient form,  $C_X(t)$ , as shown in Eq. (3), where,  $C_X(t)$  - pressure coefficient at panel  $i$ , and  $A_T$  - Total tributary area of the truss.



$$C_X(t) = \frac{X(t)}{\frac{1}{2}\rho \bar{U}_h^2 \cdot A_T} = \frac{\sum_{i=1}^N \beta_i p_i(t) A_i}{A_T} \quad (3)$$

The pressures measured simultaneously on the  $N$  panels of the truss for each approach wind direction are analyzed to obtain  $X(t)$  from which the peak value of  $C_X$  was determined. Figs. 6(a), (b) and (c) show the variation of the peak (i.e., minimum) reaction coefficients  $\check{C}_{v1}$  and  $\check{C}_{v2}$  for all five runs with the wind approach direction,  $\theta$  for trusses  $B$ ,  $F$  and  $L$  respectively and the design values obtained from AS/NZS 1170.2. The largest peak reaction on truss  $B$  occurred for  $\theta = 90^\circ$ . The values show that AS/NZS 1170.2 underestimates the reaction at  $\theta = 0^\circ$  but accommodates this for  $\theta = 90^\circ$  on truss  $B$ . Trusses  $F$  and  $L$  generally experience lower reaction forces compared to truss  $B$ .

#### 4.5. Wind load probabilistic model

Wind loads,  $W$ , acting on components of a building can be given by the probabilistic model in Eq. (4), where  $V$  is the maximum 3s gust velocity at 10 m height in standard terrain category 2 in 50 yrs (life of structure) and the parameter  $B$  includes all the other parameters including the pressure coefficients used for calculating the wind load as described by Holmes (1985) and Henderson and Ginger (2007).

$$W = BV^2 \quad (4)$$

The nominal design load is  $W_N = B_N V_N^2$  from combining the nominal values of parameters together with the wind speed. This probabilistic relationship can be presented in non dimensional form of Eq. (5)

$$[W/W_N] = [B/B_N] [V/V_N] \quad (5)$$

This normalized equation is used for the analysis of vulnerability of roofing components to wind loading discussed in Section 5.1.

#### 4.6. Dead load

The dead loads influencing each connection type are based on the weight of cladding, battens and trusses. For each connection type the dead load was calculated. The dead load can be modeled by a lognormal distribution with calculated mean value based on the material weights and an assumed coefficient of variation (0.1 was used by Holmes 1985 and Leicester *et al.* 1985)). The following values are used in this study.

$$\text{Mean } (D/D_N) = 1.05 \quad \text{COV } (D/D_N) = 0.10$$

where  $D$  - dead load,  $D_N$  -nominal value of dead load

### 5. Connection strengths and vulnerability

The components and connections in houses vary in strength (i.e., capacity) with differences in

design, materials, construction practices and workmanship. This variability exists even in connections that are designed to the same specifications and these and other uncertainties are represented in probabilistic terms.

The Cyclone Testing Station test database for a range of connection types was used to derive the statistical models for the capacity of each connection type. The particular probability distribution function (PDF) for each connection type was defined from fitting the available data to various distribution types (i.e., Normal, Lognormal, Rayleigh, Gamma and Weibull) and using the Anderson-Darling (*A-D*) goodness of fit test. The *A-D* test is particularly useful when the tails of a distribution is important. The strengths of the connections are normalized by the nominal design capacity  $\Phi R_N$  of each connection obtained from product manuals. Table 2 gives the capacity of each connection in probabilistic terms.

The lognormal distribution was found to be the best fit for all three connection strengths. It satisfied all the considered levels of significance (1%, 2%, 5%, 10% and 20%) for the cladding to batten connection. The batten to truss connection was most strongly a lognormal distribution with p-value 0.995 (the higher the p-value the stronger the assumed distribution becomes) and truss to wall connection gave a p-value of 0.58 satisfying all the confidence levels.

### 5.1. Vulnerability of roofing components

The failure of each connection type is defined as the point at which wind load exceeds the capacity of the connection. The vulnerability of components in the roof of contemporary houses located in suburban terrain (i.e., Category 2.5 in AS 4055) is determined with increasing wind speed. For wind uplift, the limit state each connection is expressed as

$$G(X) = R - (W - D) = 0 \quad (6)$$

$R$ -Structural resistance to wind uplift and  $D$  and  $W$  are dead and wind load effects respectively. Failure occurs when  $G(X) < 0$ .

The vulnerability of each connection type was assessed at selected roof locations based on Eqs. (5) and (6). The probability of failure of connections on each region was calculated for increasing steps of wind speeds by repeating the reliability analysis described in Section 2 at each wind speed. The vulnerability of cladding fastener connection, batten to truss connection and truss to wall connection are determined in selected regions of the roof for the wind approach direction generating the largest load effect (i.e., worst direction). Failure of a door or a window can create a dominant opening in contemporary houses leading to a significant increase in internal pressure. Failure of ceiling elements or the ceiling access manholes will transmit these high internal pressures to the roof cladding and as a result the wind loads on roofing components are increased. In this analysis,

Table 2 Probability distributions - connection capacity

Connection type	Mean ( $R/\phi R_N$ )	COV	PDF
Roof cladding to batten connection	1.22	0.25	Lognormal
Batten truss connection	1.46	0.30	Lognormal
Truss to wall connection	1.40	0.30	Lognormal

the percentage of houses subjected to higher internal pressure as a result of dominant opening in the envelope was taken to increase from 0% to maximum of 90% for approach gust wind speed of 40 m/s to 80 m/s. These values are based on limited survey results and the expert opinions. The internal pressure coefficient was calculated from AS/NZS1170.2. Further studies are being conducted to refine these internal pressure estimates.

Figs. 7, 8, and 9 show the vulnerability of cladding fastener connection, batten-to-truss connection and truss-to- wall connection over selected regions of the roofs for the worst directions (indicated for each region in each Figure). Fig. 7 shows that regions *P* and *Q* for cladding fixings are more vulnerable compared to the other regions. Fig. 8 shows that compared to cladding fixings, the batten to truss connections are less vulnerable and *B7* is the most vulnerable. Furthermore, Fig. 9 shows that Truss *B* near the gable end is the most vulnerable and the trusses at middle regions of the roof are less vulnerable.

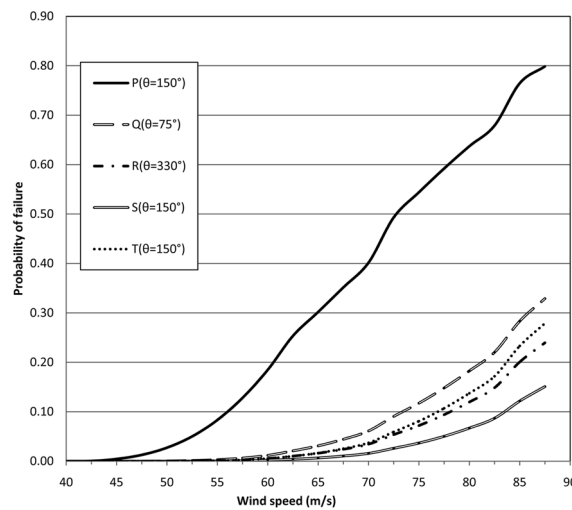


Fig. 7 Probability of failure versus wind speed - cladding connections

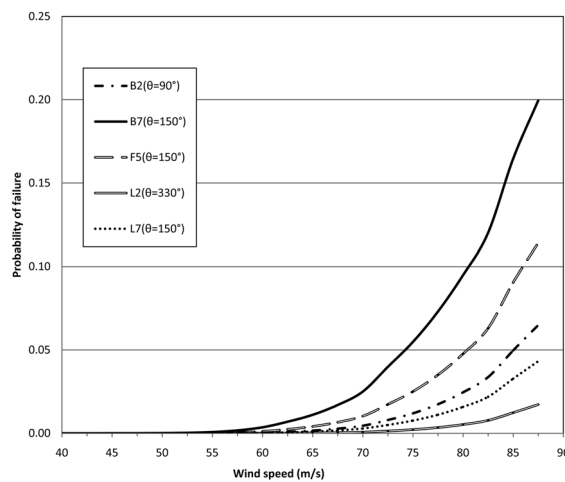


Fig. 8 Probability of failure versus wind speed - battens to truss connections

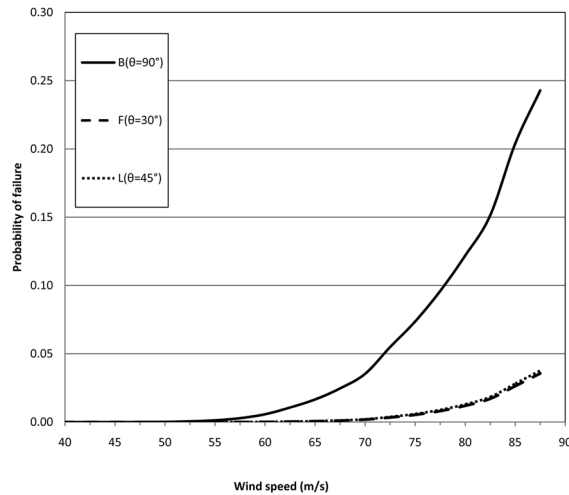


Fig. 9 Probability of failure vs Wind speed-Truss to wall connections

Fig. 10 compares vulnerabilities of cladding fastener connections in regions *P* and *Q*, between houses with dominant openings and those without. Fig. 10 shows the increased vulnerability of roofing connections when subjected to high internal pressures. This shows that the performance of houses can be improved by preventing dominant wall openings (i.e., increasing the resistance of windows and doors to debris damage).

AS/NZS 1170.2 provides information for selecting the design wind speed related to the return period. Contemporary houses are designed for 500 year return period. Fig. 11 shows the comparison of the probability of failure of the cladding fastener connection at region *P* and truss-to-wall connection of Truss *B*, with the return period (average recurrence interval) for a typical north Queensland suburban site. The results are presented for the worst direction for each connection. Similarly, the curves for each connection over the roof can be obtained for any wind approach direction. The probability of failure of these connections in a population of houses that are randomly orientated with respect to the approach wind will be much lower. These curves provide important information for structural engineers to design residential houses.

Wind pressure acting on the roofing components of a typical house described in Section 4 can be used to determine the vulnerability of roofing connections on a population of contemporary houses. The pressure coefficients on these connections will vary from house to house due to the changes in roof angle, and the basic dimensions of the houses such as width, length and height etc. The use of normalized parameters in this analysis accounts for these variations. The  $\check{C}_p/C_{pN}$  values in houses with varying dimensions will be similar to the values obtained from this wind tunnel model study. As the house dimensions vary, the corresponding values in AS/NZS1170.2 also vary correspondingly, for the connections being considered in different regions of roofs. This study used the wind pressure acting on a typical house selected from a survey. Hence, the analysis gives an accurate representation of the vulnerability of roofing connections over a population of houses subjected to largest load effect. Similarly, the vulnerability curves can be obtained for roofing connections subjected to any direction.

The vulnerability curves presented do not accommodate the overall damage to the roof, since progressive failure with increasing wind speed depends on the load sharing and interdependency of

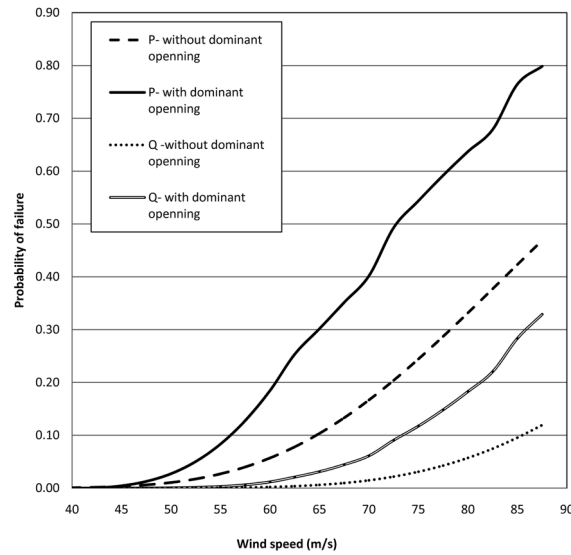


Fig. 10 Probability of failure versus wind speed - cladding connections at  $P$  and  $Q$  -worst approach direction

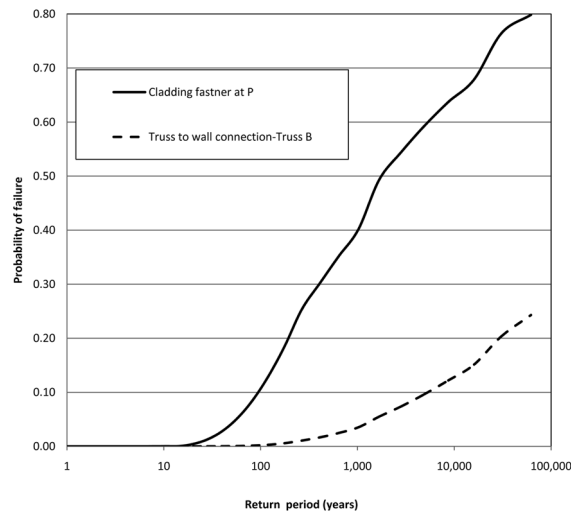


Fig. 11 Probability of failure versus return period - cladding fixing  $P$  and truss to wall connection at truss  $B$  - for the worst approach wind direction

the components/connections. The failure of one connection in the roof can prevent or increase the failure of the dependant connections (i.e., loss of roof cladding may redistribute the loads and reduce the possibility of failure of batten to truss connection failure). A companion study will conduct a range of full scale tests to study the real behavior of roofing components. In order to obtain the overall vulnerability for a population of this type of houses, the influence coefficients for various states and modes of failure will be obtained from these full scale tests and used with the individual vulnerability curves of connections. The Monte Carlo Simulation techniques will be used to obtain more detailed damage scenarios.

## 6. Conclusions

The structural system used in contemporary houses in cyclonic regions of Australia was determined from a survey of the housing stock. The wind loads on roof-cladding fixings, and batten-to-truss connection on the roof, and on the truss-to-wall connections, were determined from a wind tunnel model study on a typical contemporary house.

The study found that;

- The wind loads at the gable end and roof corners are higher compared to the middle region, and there is a large variability of the wind load on the roof of a house with the wind approach direction.
- General extreme value distribution gives the best fit for the wind loads on cladding for most of the wind approach directions.
- AS/NZS 1170.2 underestimates the external pressures on cladding fixings at gable-roof edges. However, AS/NZS 1170.2 gives a reasonable estimate for design wind loads on batten-to-truss connections, and truss-hold-down connections.
- Typical connection capacities were used to determine the roof-component strengths and probability distribution functions were best described by lognormal distributions, for all three connection types. Finally, reliability methods were applied to estimate the probability failure of cladding fixings, battens to truss connections and truss to wall connections in selected parts of the roof with increasing wind speed. The roof cladding and battens near gable ends are more vulnerable than the other regions. Furthermore, it was found that the trusses towards the gable end of the houses are more vulnerable compared to the middle of the roof.

## References

- Australian Building Codes Board (2010), Building code of Australia, ABCB, Canberra, A.C.T., Australia.
- Ellingwood, B.R., Rosowsky, D.V., Li, Y. and Kim, J.H. (2004), "Fragility assessment of light-frame construction subjected to wind and earthquake hazards", *J. Struct. Eng.-ASCE*, **130**, 1921-1930.
- Henderson, D.J. and Ginger, J.D. (2007), "Vulnerability model of an Australian high-set house subjected to cyclonic wind loading", *Wind Struct.*, **10**(3), 269-285.
- Holmes, J.D. (1981), "Wind pressures on houses with high pitched roofs", Wind Engineering Report 4/81, James Cook University, Townsville, Queensland, Australia.
- Holmes, J.D. (1985), "Wind loads and limit states design", *Civ. Eng. Trans, IE Aust.*, **27**(1), 21-25.
- Holmes, J.D. and Cochran, L.S. (2003), "Probability distributions of extreme pressure coefficients", *J. Wind Eng. Ind. Aerod.*, **91**(7), 893-901.
- Integrated Technical Software (2010), SPACE GASS, Version 10.8b, Integrated Technical Software Pty. Ltd., Geelong, Victoria, Australia.
- Kasperski, M. and Hoxey, R. (2008), "Extreme value analysis for observed peak pressures on the Silsoe cube", *J. Wind Eng. Ind. Aerod.*, **96**(6-7), 994-1002.
- Lee, K.H. and Rosowsky, D.V. (2005), "Fragility assessment for roof sheathing in high wind regions", *Eng. Struct.*, **27**(6), 857-868.
- Leicester, R.H., Pham, L. and Kleeman, P.W. (1985), "Use of reliability concepts in the conversion of codes to limit state design", *Civ. Eng. Trans, IE Aust.*, **27**, 1-7.
- Li, Q.S., Hu, S.Y., Da, Y.M. and Li, Z.N. (2009), "Extreme-value analysis for field measured peak pressure coefficients on a low-rise building", *Proceedings of the 7th Asia-Pacific Conference on Wind Engineering*, Taipei, Taiwan, November.
- Li, Y. and Ellingwood, B.R. (2006), "Hurricane damage to residential construction in the US: Importance of uncertainty modeling in risk assessment", *Eng. Struct.*, **28**(7), 1009-1018.

- Lin, J.X. and Surry, D. (1998), "The variation of peak loads with tributary area near corners on flat low building roofs", *J. Wind Eng. Ind. Aerod.*, **77-78**, 185-196.
- Melchers, R.E. (1985), "Reliability calculation for structures", *Civ. Eng. Trans. IE Aust.*, **27**(1), 124-129.
- Pham, L. (1985), "Load combinations and probabilistic load models for limit state codes", *Civ. Eng. Trans. IE Aust.*, **27**, 62-67.
- Pinelli, J.P., Simiu, E., Gurley, K., Subramanian, C., Zhang, L., Cope, A., Filliben, J.J. and Hamid, S. (2004), "Hurricane damage prediction model for residential structures", *J. Struct. Eng.-ASCE*, **130**(11), 1685-1691.
- Rosowsky, D.V. and Cheng, N. (1999), "Reliability of light frame roofs in high-wind regions. II: Wind loads", *J. Struct. Eng.-ASCE*, **125**, 734-739.
- Rosowsky, D.V. and Ellingwood, B.R. (2002), "Performance-based engineering of wood frame housing: fragility analysis methodology", *J. Struct. Eng.-ASCE*, **128**, 32-38.
- Standards Australia (2006), *Wind Loads for Housing*, Australian Standard, AS 4055-2006, Standards Australia, Sydney, N.S.W., Australia.
- Standards Australia/Standards New Zealand (2002), *Structural Design Actions – Part 2: Wind Actions*, Australian/New Zealand Standard, AS/NZS 1170.2:2002, Standards Australia, Sydney, N.S.W., Australia.
- Tang, L.K. and Melchers, R.E. (1985), "Reliability of large structural systems", *Civ. Eng. Trans. IE Aust.*, **27**, 136-142.
- Walker, G.R. (1975), "Report on cyclone track effect on buildings", Australian Dept of Housing and Construction, Canberra, A.C.T., Australia.
- Walker, G.R. (1995), "Wind vulnerability curves for Queensland houses", Alexander Howden Reinsurance Brokers (Australia) Ltd., Sydney, N.S.W., Australia.
- Xu, Y.L. and Reardon, G.F. (1998), "Variations of wind pressures on hip roofs with roof pitch", *J. Wind Eng. Ind. Aerod.*, **73**, 267-284.